Interaction of Almost-Collinear Longitudinal Phonons

H. H. Barrett and J. H. Matsinger

Raytheon Research Division, Waltham, Massachusetts

(Received 24 August 1966)

The interaction of two longitudinal ultrasonic waves to produce sum- and difference-frequency waves has been studied experimentally and theoretically. These interactions are closely analogous to the type of three-phonon interactions believed to be important in low-temperature ultrasonic attenuation. We have applied the coherent-state formalism to a description of these interactions and have discussed the similarities between coherent and incoherent processes. Experimentally we have measured the amplitude of the generated sum- or difference-frequency wave as a function of the angle between the input waves and of the amplitude and frequency of the input waves. The effect of crystalline anisotropy has also been observed. The change in amplitude of one of the input waves has been measured as a function of the parameters listed above. In all cases the experimental observations are in good agreement with theory.

I. INTRODUCTION

THE basic theory of the attenuation of ultrasonic waves through three-phonon interactions with thermal phonons has been worked out by Landau and Rumer.[1] Their theory is valid if the radian frequency ω of the ultrasonic waves times the thermal-phonon relaxation time τ_{th} is much greater than 1 since only in that case is it meaningful to speak of energy-conserving interactions involving discrete phonons. Furthermore, their results were derived for the attenuation of *transverse* waves only. They pointed out that such three-phonon interactions were unimportant in the attenuation of longitudinal ultrasonic waves because of the requirements of energy and momentum conservation. More precisely, they noted that in an isotropic dispersionless medium, a low-frequency longitudinal wave can interact with a high-frequency (thermal) longitudinal wave to produce a third longitudinal wave only if all three waves are exactly collinear. No other three-phonon interactions between a low-frequency longitudinal wave and the thermal phonons can conserve energy and momentum. Even these collinear processes are ruled out if there is dispersion of the usual type where velocity decreases with increasing frequency. Landau and Rumer therefore predict that transverse waves should be much more strongly attenuated than longitudinal waves. They also predict that the transverse attenuation should vary as ωT^4 where T is the absolute temperature.

It has recently become possible to experimentally achieve the condition $\omega\tau_{th}\gg1$ required by the Landau-Rumer theory.[2,3] The measured attenuation of transverse waves in this region is in order of magnitude agreement with the Landau-Rumer predictions and gives approximately the expected ωT^4 frequency and temperature dependence. However, the longitudinal attenuation is found to be of the same order of magni-

tude as the transverse attenuation and also to vary approximately as ωT^4. These results indicate that three-phonon processes are important for longitudinal as well as transverse wave attenuation. Simons[4] and Maris[5] have suggested an explanation for these observations. They note that exact energy conservation is not necessary for interaction with the thermal phonon because of the finite relaxation time of these phonons. Therefore, a longitudinal ultrasonic wave can interact with longitudinal thermal phonons which are only approximately collinear with it. Simons has shown that consideration of the finite relaxation time does in fact lead to an ωT^4 dependence for the longitudinal wave attenuation at least over a restricted temperature range.

In order to check the theory which has been developed for the interaction of noncollinear longitudinal phonons, the experiments reported in this paper were performed. Basically they involve passing a low-frequency and a relatively high-frequency ultrasonic wave through a solid and measuring the amplitude of the resultant sum or difference frequency wave as a function of the angle between the two primary waves. The high-frequency (~200 to 1000 Mc/sec) wave is analogous to the thermal phonons while the low-frequency wave (~7 to 50 Mc/sec) is analogous to the ultrasonic wave in an attenuation experiment. This analogy is appropriate since the condition $\omega\tau>1$ is satisfied in our experiment if ω is the radian frequency of the low-frequency wave and τ is the time available for the interaction.[6] In other words, we have scaled frequencies down and temperature up so that our interaction experiment, although performed at room temperature, satisfies the same conditions as a low-temperature ultrasonic attenuation experiment. The basic difference is that we have substituted a coherent, monochromatic and highly directional ultrasonic wave for the incoherent, random thermal phonons.

[1] L. Landau and G. Rumer, Physik. Z. Sowjetunion 11, 18 (1937).

[2] H. E. Bömmel and K. Dransfeld, Phys. Rev. 117, 1245 (1960); Phys. Rev. Letters 2, 298 (1959).

[3] H. J. Maris, Nature 198, 876 (1965).

[4] S. Simons, Proc. Phys. Soc. (London) 82, 401 (1963).

[5] H. J. Maris, Phil. Mag. 9, 901 (1964).

[6] If there is no damping, τ is obviously the time required for the input waves to propagate through the sample. The significance of τ in the presence of damping is discussed in Sec. II.

The interaction of two ultrasonic waves has been studied by a number of workers. In particular, Shiren[7] has observed the interaction of two collinear longitudinal waves at $\sim 10^{10}$ cps. However, he did not study the angular dependence of the interaction. Rollins and his co-workers[8] have studied various interactions in the low megacycle region but they specifically excluded the collinear interaction. Considerable attention has also been given to ultrasonic harmonic generation,[9-11] which is a special case of the collinear interaction. However, this paper represents the first direct observation of an "almost-collinear" acoustic-wave interaction in a solid.

II. THEORY

The classical theory of the nonlinear interaction of two elastic waves has been discussed extensively. Jones and Kobett[12] have considered the interaction of two plane waves in a homogeneous isotropic solid. They derive the momentum conservation, or "phase-matching" condition [Eq. (2.9) below] as the condition defining the direction in which the scattered wave ($\mathbf{k}_+$) is strongly peaked. They do not discuss in detail the behavior of the scattered wave in directions other than that defined by Eq. (2.9). Childress and Hambrick[13] have discussed the interaction of two elastic wave packets but again they did not consider phase mismatch.

Armstrong and his co-workers[14] have given a thorough treatment of the interaction of light waves in a nonlinear dielectric. These light-wave interactions are the direct analog of the acoustic wave interactions considered here. They derive the nonlinear coupling coefficients, or nonlinear polarizability, through a quantum-mechanical approach, but the remainder of their treatment is essentially classical. Their discussion of phase mismatch is applicable to the experiments reported here.

Shiren[15] has modified the work of Armstrong et al. so that it would apply to the collinear interaction of acoustic waves. In particular, Shiren has shown how the nonlinear coupling coefficients in the acoustic problem are related to second- and third-order elastic constants. He discusses phase mismatch due to dispersion but not due to noncollinear propagation. However, the principles are the same.

Although the specific interactions we are considering can be treated quite adequately in classical terms, a quantum-mechanical description is nonetheless useful, since it would serve to clarify the relationsip of acoustic-wave interactions to the phonon-phonon interactions observed in ultrasonic attenuation or thermal conductivity. From this viewpoint Taylor and Rollins[16] have given a quantum-mechanical treatment of the interaction of two acoustic waves. They derive a perturbation Hamiltonian from the anharmonic terms in the classical density by writing the displacement tensor as an appropriate combination of creation and annihilation operators. They then apply time-dependent "Golden rule" perturbation theory to obtain the transition probability and hence the number of phonons generated at the sum or difference frequency. They relate the number of phonons to an elastic-wave amplitude by writing the energy density of a classical elastic wave and equating it to $\eta \hbar \omega$, where η is the phonon density. In this manner they are able to reproduce the classical results obtained by Jones and Kobett. However, the validity of their procedure is not obvious. By using the golden rule, they implicitly assume that the system is initially described by an eigenstate of the unperturbed Hamiltonian. However, for a harmonic oscillator in an energy eigenstate, the expectation value[17] of the displacement $\langle x \rangle$ is identically zero regardless of the degree of excitation of the oscillator.[18] It is thus incorrect to say that the limit of a large number of phonons is a classical wave; it is only a classical wave if there is phase coherence, and phase coherence is impossible in an energy eigenstate.[19] More properly, what Taylor and Rollins have calculated is the mean-squared displacement $\langle x^2 \rangle$.

A question then arises as to what extent we can expect the results of standard perturbation theory to apply to interactions between coherent waves. This question is particularly important to the experiments described here since we hope to learn something about the interaction of a coherent ultrasonic wave and an incoherent thermal phonon by studying the interaction of two coherent waves. In particular, the observed dependence of the generated-wave amplitude on the angle of intersection of the two input waves may be described classically as an interference phenomenon. Can we expect the same "interference pattern" if one of the two waves is incoherent?

Barrett and Silverman[20] have treated this problem by using the "coherent states" of a harmonic oscillator.

[7] N. S. Shiren, Phys. Rev. Letters 11, 3 (1963).
[8] F. R. Rollins, L. H. Taylor, and P. H. Todd, Phys. Rev. 136, A597 (1964).
[9] M. A. Breazeale and J. Ford, J. Appl. Phys. 36, 3486 (1965).
[10] P. H. Carr, Phys. Rev. Letters 13, 332 (1964).
[11] A. Hikata, B. B. Chick, and C. Elbaum, J. Appl. Phys. 36, 229 (1965).
[12] G. L. Jones and D. R. Kobett, J. Acoust. Soc. Am. 35, 5 (1963).
[13] J. D. Childress and C. G. Hambrick, Phys. Rev. 136, A411 (1964).
[14] J. Armstrong, N. Bloembergen, J. Ducuing, and P. Pershan, Phys. Rev. 127, 1918 (1962).
[15] N. S. Shiren, Proc. IEEE 53, 1540 (1965).

[16] L. Taylor and F. R. Rollins, Phys. Rev. 136, A591 (1964).
[17] It is important to distinguish here between time averages and quantum-mechanical expectation values. The latter are denoted by $\langle \ \rangle$.
[18] P. Carruthers and M. M. Nieto, Am. J. Phys. 33, 537 (1965).
[19] P. Carruthers and M. M. Nieto, Phys. Rev. Letters 14, 387 (1965).
[20] H. H. Barrett and B. D. Silverman, Bull. Am. Phys. Soc. 11, 259 (1966).

These states have been discussed in detail by Glauber[21] in connection with coherent photon fields. If the lattice vibrations in a crystal are resolved into harmonic oscillator normal modes, specified by a wave vector $\mathbf{k}$ and a polarization index μ, then the lattice displacement $\mathbf{x}(\mathbf{r},t)$ at the point $\mathbf{r}$ and time t is described in the Heisenberg picture by the operator[22]

$$\mathbf{x}(\mathbf{r},t)=\sum_{\mathbf{k},\mu}\mathbf{e}(\mathbf{k},\mu)[2\rho\omega(\mathbf{k},\mu)]^{-1/2}$$
$$\times\{a(\mathbf{k},\mu)\exp i[\mathbf{k}\cdot\mathbf{r}-\omega(\mathbf{k},\mu)t]$$
$$+a^\dagger(\mathbf{k},\mu)\exp-i[\mathbf{k}\cdot\mathbf{r}-\omega(\mathbf{k},\mu)t]\}. \quad (2.1)$$

Here $\mathbf{e}(\mathbf{k},\mu)$ is a unit vector in the direction of the polarization of the phonon, ρ is the mass density, $\omega(\mathbf{k},\mu)$ is the frequency of the mode, and $a(\mathbf{k},\mu)$ and $a^\dagger(\mathbf{k},\mu)$ are the usual boson annihilation and creation operators. Since we will be concerned with only longitudinal waves, we will drop the polarization index μ. The frequency and wave vector are related by $\omega(\mathbf{k})=v|\mathbf{k}|$, where v is the phase velocity for the mode. A coherent state for mode $\mathbf{k}$ is then an eigenstate of $a(\mathbf{k})$

$$a(\mathbf{k})|\beta(\mathbf{k})\rangle=\beta(\mathbf{k})|\beta(\mathbf{k})\rangle, \quad (2.2)$$

where

$$\beta(\mathbf{k})=|\beta(\mathbf{k})|e^{i\phi(\mathbf{k})} \quad (2.3)$$

specifies the amplitude and phase $\phi(\mathbf{k})$ of the excitation.

These coherent states do not form an orthogonal set of states, but they do form a complete (in fact, over-complete) set. Therefore, an arbitrary state may be expanded in terms of coherent states and the expansion may be inverted. In particular, Glauber has given the expansion of a coherent state in terms of energy eigenstates $|n(\mathbf{k})\rangle$

$$|\beta(\mathbf{k})\rangle=\sum_{n(\mathbf{k})}\frac{e^{-(1/2)|\beta(\mathbf{k})|^2}[\beta(\mathbf{k})]^{n(\mathbf{k})}}{[n(\mathbf{k})!]^{1/2}}|n(\mathbf{k})\rangle, \quad (2.4)$$

where

$$a^\dagger(\mathbf{k})a(\mathbf{k})|n(\mathbf{k})\rangle=n(\mathbf{k})|n(\mathbf{k})\rangle \quad (2.5)$$

and $n(\mathbf{k})$ is the total number of phonons in the mode $\mathbf{k}$.

If mode $\mathbf{k}$ is excited to a coherent state $|\beta(\mathbf{k})\rangle$ and all other modes have only incoherent (e.g., thermal) excitation, the term in the lattice displacement operator associated with mode $\mathbf{k}$ has the expectation value

$$\langle x(\mathbf{k};\mathbf{r},t)\rangle=x_0(\mathbf{k})|\beta(\mathbf{k})|\cos[\mathbf{k}\cdot\mathbf{r}-\omega(\mathbf{k})t+\phi(\mathbf{k})], \quad (2.6)$$

where

$$x_0(\mathbf{k})\equiv2\mathbf{e}(\mathbf{k})[2\rho\omega(\mathbf{k})]^{-1/2}. \quad (2.7)$$

Barrett and Silverman assumed that two modes, $\mathbf{k}_1$ and $\mathbf{k}_2$, were excited to the coherent amplitudes $\beta(\mathbf{k}_1)$

and $\beta(\mathbf{k}_2)$, respectively, at time t. They then took as a perturbing Hamiltonian

$$H_1=g_+a(\mathbf{k}_+)a^\dagger(\mathbf{k}_1)a^\dagger(\mathbf{k}_2)+g_+{}^*a^\dagger(\mathbf{k}_+)a(\mathbf{k}_1)a(\mathbf{k}_2)$$
$$+g_-a(\mathbf{k}_-)a(\mathbf{k}_1)a^\dagger(\mathbf{k}_2)+g_-{}^*a^\dagger(\mathbf{k}_-)a^\dagger(\mathbf{k}_1)a(\mathbf{k}_2), \quad (2.8)$$

where $g_\pm$ may be simply related to the anharmonic properties of the medium.[15] Note that $g_\pm$ vanishes unless

$$\mathbf{k}_2\pm\mathbf{k}_1=\mathbf{k}_\pm. \quad (2.9)$$

We have assumed that $\omega(\mathbf{k}_2)>\omega(\mathbf{k}_1)$. In general H_1 should include other terms, such as harmonic generation terms, but these are unimportant for our present purposes.

The interaction is "turned on" at time t and at a later time $t+\tau$ there will be an excitation in the sum- and difference-frequency modes, $\mathbf{k}_\pm$, given to first-order perturbation theory by

$$\langle x(\mathbf{k}_\pm;\mathbf{r},t+\tau)\rangle=x_0(\mathbf{k}_\pm)|g_\pm|\cdot|\beta(\mathbf{k}_1)|\cdot|\beta(\mathbf{k}_2)|$$
$$\times\sin[\mathbf{k}_\pm\cdot\mathbf{r}-(\omega_2\pm\omega_1)(t+\tau)+\Phi-\tfrac{1}{2}\Delta\omega_\pm\tau]$$
$$\times(\sin\tfrac{1}{2}\Delta\omega_\pm\tau/\tfrac{1}{2}\hbar\Delta\omega_\pm), \quad (2.10)$$

where $\omega_2\equiv\omega(\mathbf{k}_2)$ and $\omega_1\equiv\omega(\mathbf{k}_1)$. Φ depends on the phases of $\beta(\mathbf{k}_1)$, $\beta(\mathbf{k}_2)$, and $g_\pm$, while $\Delta\omega_\pm$ is defined by

$$\Delta\omega_\pm=\omega_2\pm\omega_1-\omega(\mathbf{k}_\pm). \quad (2.11)$$

Note that $\omega(\mathbf{k}_\pm)\equiv v|\mathbf{k}_\pm|$ and is not exactly the sum or difference frequency unless $\mathbf{k}_1$ and $\mathbf{k}_2$ are parallel. However, $\langle x(\mathbf{k}_\pm;\mathbf{r},t+\tau)\rangle$ oscillates at the frequency $\omega_2\pm\omega_1$ and not at $\omega(\mathbf{k}_\pm)$, which is the natural frequency of the mode $\mathbf{k}_\pm$. The process may be thought of as a driven harmonic oscillator. The term $\tfrac{1}{2}\Delta\omega_\pm\tau$ in the argument of the first sine function in Eq. (2.10) is simply a phase shift arising during the interaction.

The factor

$$F=\sin\tfrac{1}{2}\Delta\omega_\pm\tau/\tfrac{1}{2}\Delta\omega_\pm \quad (2.12)$$

is the square root of the usual energy-conservation factor which occurs in Golden-rule perturbation theory. The square root appears since we are calculating amplitude rather than energy. For exact energy conservation ($\Delta\omega_\pm=0$), F grows linearly with the interaction time τ; for $\Delta\omega_\pm\neq0$, F oscillates sinusoidally with τ.

In the Appendix, $\Delta\omega_\pm$ is related to the angle θ between the two input waves. It is shown that if $\omega_2\gg\omega_1$,

$$\Delta\omega_\pm\approx(\tfrac{1}{2}-b)\omega_1\theta^2, \quad (2.13)$$

where b is an anisotropy parameter defined in the Appendix ($b=0$ for an isotropic medium). Then the amplitude of the generated signal at the sum or difference frequency should have an angular dependence given by

$$F=\mathrm{sinc}\omega_1\theta^2\tau/c\omega_1\theta^2, \quad (2.14)$$

where $c\equiv\tfrac{1}{2}(\tfrac{1}{2}-b)$ is a constant calculable from the elastic constants of the material.

[21] R. J. Glauber, Phys. Rev. **131**, 2766 (1963).
[22] C. Kittel, *Quantum Theory of Solids* (John Wiley & Sons, Inc., New York, 1963), p. 23.

Another quantity of interest, because of its close connection with ultrasonic attenuation, is the change in amplitude of the input wave due to the interaction. By going to second-order perturbation theory, Barrett and Silverman obtain the following results:

$$|\beta(\mathbf{k}_1, t+\tau)| = |\beta(\mathbf{k}_1, t)| [1 + \tfrac{1}{2}\hbar^{-2}|g_-|^2 (n_2 - n_-)F^2 - \tfrac{1}{2}\hbar^{-2}|g_+|^2 (n_2 - n_+)F^2], \quad (2.15)$$

$$|\beta(\mathbf{k}_2, t+\tau)| = |\beta(\mathbf{k}_2, t)| [1 - \tfrac{1}{2}\hbar^{-2}|g_-|^2$$
$$\times (n_- + n_1 + 1)F^2 - \tfrac{1}{2}\hbar^{-2}|g_+|^2$$
$$\times (n_1 - n_+)F^2], \quad (2.16)$$

where $|\beta(\mathbf{k}_i, t)|$ is the amplitude of the coherent excitation in mode $\mathbf{k}_i$, F is defined by Eq. (2.12) or Eq. (2.14), n_i is the average number of quanta in mode $\mathbf{k}_i$ at the initial time t, and $n_\pm$ is the number in mode $\mathbf{k}_\pm$. In general n_i is defined as $\langle a^\dagger(\mathbf{k}_i)a(\mathbf{k}_i)\rangle$ at time t and will include both the coherent excitation and any incoherent excitation which may be present.

In most cases the modes $\mathbf{k}_\pm$ will be unpopulated at time t except for thermal phonons while modes $\mathbf{k}_1$ and $\mathbf{k}_2$ will be driven to an occupation number much in excess of the thermal value. Under these circumstances we may neglect n_- or n_+ compared to n_1 or n_2. Then we see that Eqs. (2.15) and (2.16) predict that difference-frequency interactions (terms involving $|g_-|^2$) will lead to a gain in amplitude in mode $\mathbf{k}_1$ and a loss in mode $\mathbf{k}_2$ (note that $\omega_2 > \omega_1$), while sum-frequency interactions lead to loss in both modes. In general $|g_+|$ will be slightly greater than $|g_-|$ so there will be a net loss in both modes. Note that the change in amplitude of one of the input waves, $\Delta|\beta(\mathbf{k}_i)|$, should be proportional to the amplitude of that wave and to the square of the amplitude of the other input wave, since, neglecting thermal excitation, $n_j = |\beta(\mathbf{k}_j)|^2$. (We are assuming that $n_\pm$ is also small.) Also $\Delta|\beta(\mathbf{k}_i)|$ should be proportional to F^2, while $|\beta(\mathbf{k}_\pm)|$ was found to be proportional to F. Experimental verification of these features is presented in Sec. IV.

Having discussed the coherent-state treatment of the problem of two interacting ultrasonic waves, we may now compare it to the Golden-rule perturbation-theory treatment employed by Taylor and Rollins. If we consider both the sum-frequency generation process and its inverse, where a phonon in mode $\mathbf{k}_+$ decays into a phonon in mode $\mathbf{k}_1$ and a phonon in mode $\mathbf{k}_2$, standard perturbation theory tells us that the net transition probability per unit time is proportional to

$$|g_+|^2 F^2 [n_1 n_2 (n_+ + 1) - (n_1 + 1)(n_2 + 1)n_+]$$
$$= |g_+|^2 F^2 [n_1(n_2 - n_+) - n_+(n_2 + 1)]$$
$$\approx |g_+|^2 F^2 n_1 n_2. \quad (2.17)$$

The last form of Eq. (2.17) obviously results from assuming that n_+, the initial population of mode $\mathbf{k}_+$, is negligible compared to n_1 and n_2. In this approximation

Eq. (2.17) is equivalent to[23] Eq. (2.10), which may be rewritten

$$|\beta(\mathbf{k}_+)|^2 = (1/\hbar^2)|g_+|^2 F^2 |\beta(\mathbf{k}_1)|^2 |\beta(\mathbf{k}_2)|^2. \quad (2.18)$$

However, Eq. (2.10) is more general than Eq. (2.17), since the former equation was derived without any assumption about the values of n_1, n_2, or $n_\pm$; the only assumption made was that the *coherent part* of the excitation in modes $\mathbf{k}_\pm$ was zero (which does not imply that $n_\pm$ was zero). This is the real advantage of the coherent-state theory: Coherent and incoherent excitations may be included on the same basis without any special assumptions about their relative magnitudes, and the contribution of each type of excitation to the process of interest is clearly displayed. Thus, for example, Eq. (2.15) shows that the coherence of the $\mathbf{k}_2$ is unimportant[24] in determining $\Delta|\beta(\mathbf{k}_1)|$. However, Eq. (2.17) correctly expresses the energy change $\hbar\omega_1 \Delta n_1(t+\tau)$. The difference between n_1 and $|\beta(\mathbf{k}_1)|^2$ is the noise in the system, including thermal noise and spontaneous emission. A further advantage of the coherent-state method is that it provides the possibility for the calculation of purely quantum-mechanical effects, such as spontaneous emission or quantum noise, and it often leads to a considerable simplification of the algebra, especially when both coherent and incoherent excitations are present.[25]

In the foregoing discussion we have assumed that the interaction is switched on abruptly at time t and the system is observed at time $t+\tau$. We have also assumed that the amplitudes of the input waves are essentially constant during this period, i.e., $\Delta|\beta(\mathbf{k}_i)| \ll |\beta(\mathbf{k}_i)|$, $(i=1, 2)$. However, in the experiments described in this paper there is always some attenuation of the input waves (other than that resulting from the interaction between them) so the latter assumption is not always justified. We will now investigate the generation of sum and difference frequencies in a lossy nonlinear medium.

From the coherent perturbation theory treatment leading to Eq. (2.10), it can readily be shown that, in the absence of damping, the coherent amplitude in mode

---

[23] The reason for the success of the Golden-rule approach in this approximation may be seen from Eq. (2.4). We could have decomposed the coherent input waves into a Poisson distribution of energy eigenstates. For large values of n_1 and n_2 the Poisson distributions are relatively narrow (widths $\sqrt{n_1}$ and $\sqrt{n_2}$, respectively) so that the *energy* in mode $\mathbf{k}_\pm$ builds up just as if the input waves were pure energy eigenstates. However, calculation of the coherence properties of the generated wave by this procedure would require going to higher order perturbation theory since, in first order, the vacuum state for mode $\mathbf{k}_\pm$ is connected only to the one-phonon state.

[24] Thus, Eq. (2.15) shows quantum mechanically the possibility of an acoustic parametric amplifier with an incoherent pump, as discussed by Shiren (Ref. 15).

[25] A case where it may be particularly important to distinguish between coherent and incoherent excitation is the phonon bottleneck problem in ultrasonic attenuation. See J. DeKlerk, D. I. Bolef, and P. G. Klemens, Phys. Rev. Letters 10, 127 (1963).

k_- at time $t+\Delta t$ is related to its value at time t by

$$\beta(k_-, t+\Delta t)=\beta(k_-,t)-\frac{i}{\hbar}g_-^*\beta^*(k_1,t)\beta(k_2,t)$$

$$\times\int_t^{t+\Delta t}\exp(-i\Delta\omega_-t')dt'. \quad (2.19)$$

Equation (2.19) is valid only if $\beta^*(k_1,t)$ and $\beta(k_2,t)$ do not change appreciably in a time interval Δt. To account for a general variation of these amplitudes, we may take Δt to be infinitesimally small. So, replacing Δt by dt, we obtain

$$\frac{d\beta(k_-,t)}{dt}\bigg|_{int}=-\frac{i}{\hbar}g_-^*\beta^*(k_1,t)\beta(k_2,t)\exp(-i\Delta\omega_-t). \quad (2.20)$$

If the time dependence of $\beta^*(k_1,t)$ and $\beta(k_2,t)$ is due to damping, we may write

$$\beta^*(k_1,t)=\beta^*(k_1,0)\exp(-\gamma_1 t),$$
$$\beta(k_2,t)=\beta(k_2,0)\exp(-\gamma_2 t), \quad (2.21)$$

where we assume the variation of these amplitudes due to sum- or difference-frequency production is small compared to the damping from other mechanisms. Now Eq. (2.20) describes only the generation of coherent excitation in mode k_-; we must add a term describing the damping of this mode

$$\frac{d\beta(k_-,t)}{dt}=\frac{d\beta(k_-,t)}{dt}\bigg|_{int}-\gamma_-\beta(k_-,t). \quad (2.22)$$

Obviously, if the interaction is switched off, $\beta(k_-)$ will decay exponentially with a time constant $(\gamma_-)^{-1}$. Presumably γ_1, γ_2, and γ_- may be measured independently. Solving Eq. (2.22) subject to the boundary condition $\beta(k_-,0)=0$, we find that after interacting for a time τ,

$$|\beta(k_-,\tau)|=(1/\hbar)|g_-|\cdot|\beta(k_1,0)|$$

$$\times|\beta(k_2,0)|\exp[-\tfrac{1}{2}(\gamma_1+\gamma_2)\tau]$$

$$\times\left[\frac{\sinh^2\tfrac{1}{2}\gamma\tau+\sin^2\tfrac{1}{2}\Delta\omega_-\tau}{(\tfrac{1}{2}\gamma)^2+(\tfrac{1}{2}\Delta\omega_-)^2}\right]^{1/2}, \quad (2.23)$$

where
$$\gamma\equiv\gamma_1+\gamma_2-\gamma_-. \quad (2.24)$$

We may define

$$F'=N\left[\frac{\sinh^2\tfrac{1}{2}\gamma\tau+\sin^2\tfrac{1}{2}\Delta\omega_-\tau}{(\tfrac{1}{2}\gamma)^2+(\tfrac{1}{2}\Delta\omega_-)^2}\right]^{1/2}, \quad (2.25)$$

where N is a normalizing factor chosen to make $F'=1$ when $\Delta\omega_-=0$. If $\gamma=0$, F' reduces to F as defined by Eq. (2.12). Figure 1 is a plot of F' as a function of $\Delta\omega_-\tau$ for various values of $\gamma\tau$. Note that F' does not differ appreciably from F unless $\gamma\tau>1$. In all of the experiments reported here, $\omega_1\ll\omega_2$ and $\omega_\pm\approx\omega_2$. There-

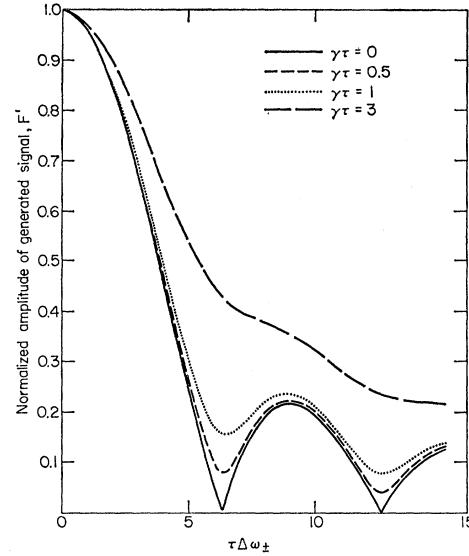FIG. 1. Theoretical dependence of the generated sum- or difference-frequency amplitude on energy uncertainty. τ is the transit time across the specimen and γ is defined as $\gamma_1+\gamma_2-\gamma_\pm$, where γ_i is the damping constant of mode k_i. The generated signal amplitude is normalized to its value when $\Delta\omega=0$.

fore, $\gamma_1\ll\gamma_2$ and $\gamma_2\approx\gamma_\pm$ since the acoustic attenuation increases with frequency. Thus even if $\gamma_2\tau>1$, it is still possible that $\gamma\tau\ll1$ so that F' will be nearly indistinguishable from F. Equation (2.23) holds for sum frequency generation also. However, γ will be identically zero for sum-frequency generation if the acoustic attenuation is a linear function of frequency.

III. EXPERIMENTAL APPARATUS

The apparatus used in these experiments is shown schematically in Fig. 2. The high-frequency (hf) ultrasonic wave is generated by a transducer attached directly to the sample. This transducer was a CdS film for most of the measurements reported here, but a 10 Mc/sec X-cut quartz transducer operated at a high harmonic has also been used. The low-frequency (lf) wave is generated by a 1 in.-diam X-cut quartz plate with a fundamental resonant frequency of about 7 Mc/sec. The lf wave travels through the water and a portion of it is transmitted into the sample. Both signals are pulses, and they are timed to arrive at the water-sample interface simultaneously. The transmitted component of the lf wave and the reflected component of the hf wave then travel down the sample together. The angle between the two waves may be varied since the lf transducer is mounted on a goniometer. The direction of the lf wave in the water may be measured to an accuracy of better than 5 min of arc, and its direction in the sample may then be computed from Snell's law. The sample end faces are flat to $\frac{1}{10}$ wavelength of sodium light and parallel to 10 sec of arc.
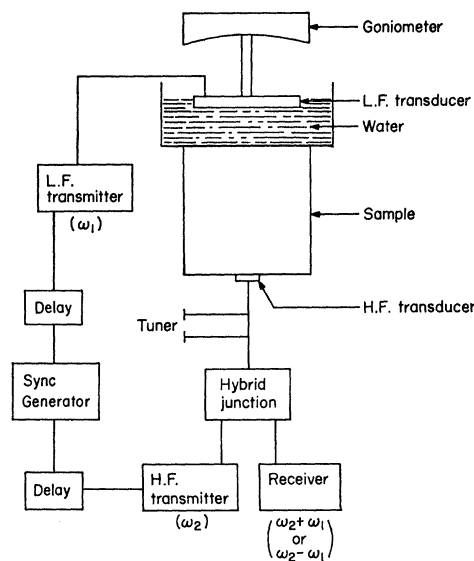
As the two waves travel together through the sample,

FIG. 2. Apparatus used to observed generated sum or difference frequencies.

they interact and produce sum- and difference-frequency waves. These generated waves are detected by the same transducer that produced the hf wave. The relative amplitude of the sum- or difference-frequency signal is measured by means of a calibrated attenuator in the receiver. When a quartz plate is used for the hf transducer, the lower frequency f_1 is restricted to be an *even* multiple of the hf transducer fundamental frequency so that the hf transducer can both generate frequency f_2 and detect $f_2 \pm f_1$. This restriction is not necessary with CdS film transducers since they usually have a bandwidth of several hundred megacycles.

The lf transducer is large in diameter in order to reduce the angular beam spread due to diffraction, which results in the interaction taking place within the near field of the lf transducer. However, all of the measurements can be adequately explained in terms of plane waves, probably because the rapid amplitude variations in the near field average out over the interaction volume.

The diameter of the active area of the hf transducer is quite critical. It must be large enough so that there will be no appreciable angular spread due to diffraction and yet small enough to have a nearly uniform response to the generated wave as the interaction angle is varied. That this is possible may be seen as follows: Referring to Fig. 3, the relative response of a circular transducer of radius a to a plane wave of wave vector $\mathbf{k}$ incident at an angle ψ is given by

$$R = 2J_1(ka \sin\psi)/ka \sin\psi, \qquad (3.1)$$

where $k = |\mathbf{k}| = \omega/v$, ω is the radian frequency of the wave and v is its phase velocity. R will be recognized as the far-field diffraction pattern of a circular piston.

Now, as discussed in the last section, the interaction must obey the wave-vector conservation condition

$$\mathbf{k} = \mathbf{k}_{\pm} = \mathbf{k}_2 \pm \mathbf{k}_1, \qquad (3.2)$$

where $\mathbf{k}_{\pm}$ refers to the generated wave, $\mathbf{k}_1$ and $\mathbf{k}_2$ refer to the lf and hf input waves, respectively, and the plus or minus signs are for sum or difference frequency processes, respectively. Note that $\mathbf{k}_2$ is normal to the hf transducer. Applying the law of sines to the wave-vector conservation triangle for sum-frequency generation (see Fig. 3), R for the generated wave may be written as

$$R = 2J_1(k_1 a \sin\theta)/k_1 a \sin\theta. \qquad (3.3)$$

In other words, the response of the hf transducer to the generated wave is exactly the same as it would be to the lf input wave if it were detected directly by the hf transducer. If f_2 is increased, the generated frequency is also increased, but its angle of incidence ψ is decreased and the transducer response is unchanged. This conclusion is also valid for difference-frequency generation. Thus the radius a of the hf transducer is chosen to minimize the angular spread of the hf wave due to diffraction and f_1 is kept sufficiently small so that $R \approx 1$ at the largest angle of interest. In practice it has been convenient to adjust the radius by using a small spot of conducting paint to define the active area of the hf transducer.

The electronics used is fairly conventional. The lf transmitter is an Arenberg pulsed oscillator. The hf transmitter is a tuned-grid, tuned-cathode pulsed oscillator which covers most of the range from 180 to 950 Mc/sec and which delivers several hundred watts of rf power. The superheterodyne receiver employs a balanced-diode mixer and has a sensitivity of about -100 dBm.

Although the amplitude of the generated sum- or difference-frequency wave is of considerable theoretical interest, it is the change in amplitude of the input wave (due to the interaction) which is most nearly analogous to ultrasonic attenuation. The system we have used to measure this change is shown schematically in Fig. 4. The lf transmitter is triggered at a 500-cps rate while

(a) Sum frequency geometry   (b) Difference frequency geometry
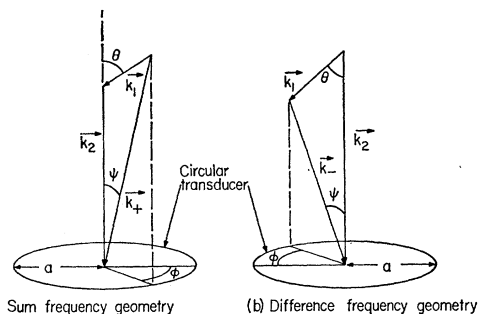
FIG. 3. Illustration of interaction geometry. (a) Sum-frequency generation, (b) difference-frequency generation.
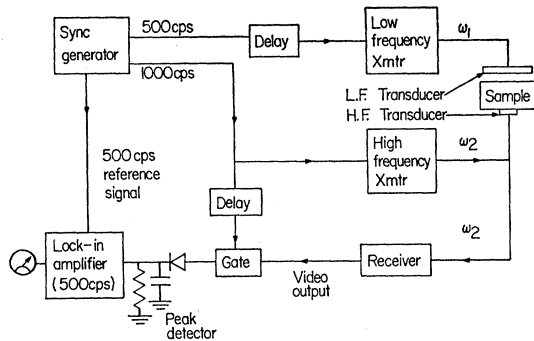
FIG. 4. Apparatus used to observe change in amplitude of input wave.

the hf transmitter is triggered at 1000 cps. The attenuation in the sample is sufficiently large that all of the ultrasonic energy in the sample decays within 1 msec. Thus, only the echos resulting from every other hf transmitter pulse are affected by the interaction. The gate following the receiver video output serves to select a particular hf echo, usually the first, from each sequence of echos. Alternate pulses out of this gate will then be reduced in amplitude by the interaction. The peak detector and lock-in amplifier respond linearly to the difference in amplitude of successive pulses, and therefore give a direct measure of the strength of the interaction. With this system amplitude changes as small as 0.002 dB may be detected.

IV. EXPERIMENTAL RESULTS AND DISCUSSION

The production of acoustic sum- and difference-frequency waves by the interaction of two longitudinal acoustic waves has been observed in a variety of materials, including ruby, rutile, strontium titanate, silicon, fused quartz, and calcium tungstate. However, most of the quantitative measurements have been confined to silicon and fused quartz. With these two materials the nonlinearities were sufficiently great that the sum- or difference-frequency signal was typically 30–40 dB above noise (with the input waves parallel) and of the order of 40 dB weaker than the hf input signal. No careful measurements of the conversion efficiency were made since it was not our purpose to study the origin or magnitude of the nonlinearities.

Since the angular response of the hf transducer can seriously affect the observed angular dependence in this experiment, it is important to establish experimentally the validity of the assumption that $R \approx 1$ [see Eq. (3.3)]. This may be done by plotting the observed angular width of the interaction at some reference amplitude as a function of $1/\sqrt{f_1}$, where $f_1 \equiv \omega_1/2\pi$ is the lower input frequency. Referring to Eq. (2.14), it may be seen that choosing a reference amplitude is equivalent to setting $\omega_1\theta^2\tau$ equal to a constant. Therefore, a plot of the angle θ_{ref} required to give this reference amplitude versus $1/\sqrt{f_1}$ should

yield a straight line. However, if the observed angular width is determined by the transducer response rather than by the characteristics of the bulk interaction, such a plot will be a parabola as may be seen by setting Eq. (3.3) equal to a constant. Any deviation from linearity in these plots will then be an indication that $R \neq 1$. A typical $1/\sqrt{f_1}$ plot is shown in Fig. 5. These plots are used routinely as a diagnostic tool to determine the influence of the transducer response. Incidentally a plot such as Fig. 5 is also proof that the observed interaction is taking place in the bulk of the material. If it was occurring on the surface of the hf transducer or in the external circuitry, the angular dependence would be the same as the angular response of the transducer.

Figure 6 shows the dependence of the difference-frequency amplitude on the angle between the two input waves as observed in a silicon sample. This sample was a right circular cylinder 4.35 cm long and 2.2 cm in diam. The [111] crystallographic axis was parallel to the axis of the cylinder (and therefore parallel to k_2). The material was 6-Ω cm, N-type, Sb-doped silicon obtained from Texas Instruments Company. The theoretical curve in Fig. 5 is simply a plot of the factor F from Eq. (2.14), using the measured value of the transit time τ and using the value of c calculated from expressions given by Waterman.[26] It is seen that the agreement with theory for angles less than about 9° is quite good. For larger angles the agreement is poorer, as at about ±11°. There are several reasons for discrepancies at large angles. First, as discussed in Sec. III, the hf transducer response varies with angle of incidence and the approximation that $R \approx 1$ begins to fail at large angle. Also the trans-
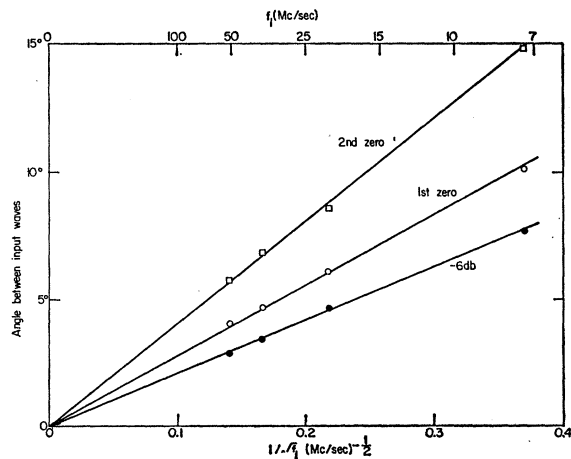

FIG. 5. The angle between the input waves required to give the specified relative amplitude for the generated difference frequency signal as a function of $1/\sqrt{f_1}$, where f_1 is the lower input frequency. The straight lines are the theoretical dependence. The sample was fused quartz and the higher input frequency was 250 Mc/sec.

[26] P. C. Waterman, Phys. Rev. 113, 1240 (1959).

mission coefficient at the water-sample interface may vary somewhat with angle. Finally, at large angles the signal level is low and noise is beginning to affect the accuracy of the measurements. The largest effect is undoubtedly the transducer response. However, none of these difficulties influence appreciably the determination of the zeros of the interaction, i.e., the angles at which the generated signal vanishes.[27] Therefore, more significance can be attached to the position of these zeros than to other large-angle points. Note that in Fig. 6 the three zeros which were observed on either side of the main lobe agree quite well with theory.

Figure 7 shows similar data for a fused-quartz sample. In this case the specimen was a cylinder 5.08 cm long and 2.54 cm in diameter. It was obtained from the General Electric Company, Willoughby Quartz Plant. At least five minima were observed on either side of the main lobe with this sample. Their positions were quite close to theoretical predictions. The theoretical curve in Fig. 7 is a plot of the factor F' [from Eq. (2.25)] rather than F, since the losses in fused quartz are fairly large. However, the angular resolution of the experiment was insufficient to determine whether F or F' fit the data better. In all of the measurements the effect of loss on the angular dependence was unobservable, even though in some cases $\gamma_2 \tau$ was about 2.

In the Appendix we show that $\Delta \omega_\pm$ depends on the elastic anisotropy of the medium through a factor $(\frac{1}{2} - b)$ where expressions for b in terms of the elastic constants of the material have been given by Waterman.[26] The parameter b can take on both positive and negative values so anisotropy can act to either increase or decrease the angular range over which the interaction can occur. In particular if b approaches $\frac{1}{2}$, this inter-

FIG. 7. Angular dependence of difference-frequency amplitude in fused quartz. Input frequencies were 300 and 20.6 Mc/sec. The theoretical curve is a plot of the factor F' defined by Eq. (2.25).

action can occur at very large angles and its contribution to longitudinal ultrasonic attenuation is correspondingly increased. This point has been discussed in detail by Barrett,[28] who used Eq. (2.13) for $\Delta \omega_\pm$ as his starting point. He showed that in some anisotropic materials the calculated attenuation can differ by as much as a factor of 7 from the attenuation calculated for an isotropic but otherwise identical material. Therefore it is of some interest to experimentally verify Eq. (2.13). It would be particularly valuable to verify Waterman's expressions for b since his paper has been used as the basis for other work[29–31] but has not, to the authors's knowledge, been submitted to a direct experimental test.

In order to directly observe the effects of elastic anisotropy, we have studied the almost-collinear interaction of two longitudinal acoustic waves propagating close to a [110] axis in silicon. In this case Waterman's results indicate that b depends on the azimuthal angle ϕ of $\mathbf{k}_1$ in a spherical coordinate system in which $\mathbf{k}_2$ is parallel to the z axis (see Fig. 3); if the z axis is a [110] axis, his results may be stated

$$b = -A \cos^2\phi - B \sin^2\phi, \qquad (4.1)$$

where, for silicon, A and B have the values -0.236 and 0.185, respectively. Let θ_0 denote the angle between $\mathbf{k}_1$ and $\mathbf{k}_2$ at the first zero of the function F. Then

$$\tfrac{1}{2}\Delta\omega_\pm \theta_0^2 \tau = \pi \qquad (4.2)$$

or

$$\theta_0 = \left[\frac{4\pi}{\omega_1\tau(1 + 2A\cos^2\phi + 2B\sin^2\phi)} \right]^{1/2}. \qquad (4.3)$$

Our results for θ_0 as a function of ϕ are given in the form of a polar plot in Fig. 8. The angle θ_0 is the *radius* of the polar plot while ϕ is the polar angle in the plot.
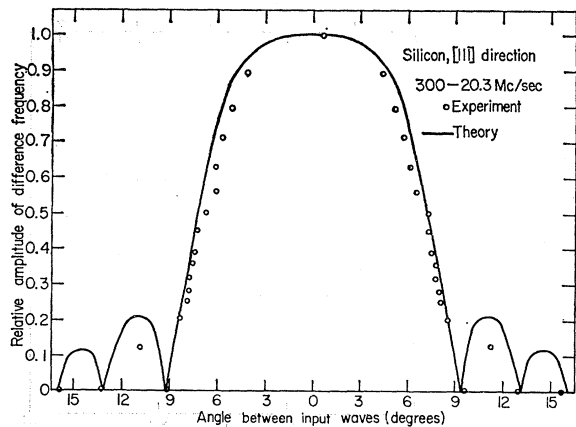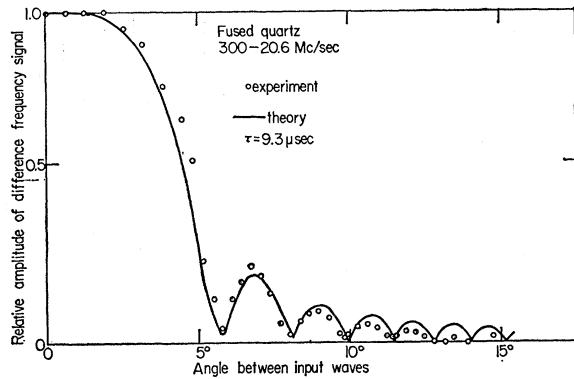

FIG. 6. Angular dependence of difference-frequency amplitude in [111] silicon. Input frequencies were 300 and 20.3 Mc/sec. Note agreement with theory at the zeros of the theoretical function.

---

[27] However the transducer response can introduce spurious zeros. Also both input transducers contribute a small but finite angular spread due to diffraction so that we usually did not observe true zeros, but rather minima.

[28] H. H. Barrett, Phys. Letters 21, 623 (1966).
[29] E. P. Papadakis, J. Acoust. Soc. Am. 36, 414 (1964).
[30] R. A. Artman, J. Acoust. Soc. Am. 39, 493 (1966).
[31] H. J. McSkimin and W. Bond, J. Acoust. Soc. Am. 39, 499 (1966).
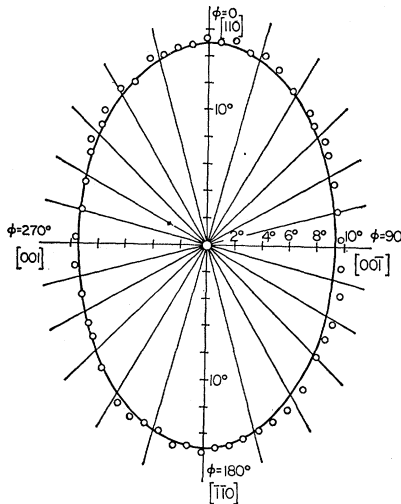
LONGITUDINAL PHONONS

FIG. 8. Polar plot of the angular width of the interaction showing the elastic anisotropy in silicon. The radius in this plot is the angle between the input waves required to make the generated signal amplitude equal zero (the first zero in a plot such as Fig. 5 or 6). The angle ϕ is the azimuthal angle of k_1 in spherical coordinates when k_2 is taken as the z axis. k_2 is parallel to the [110] axis of the sample. For example, when $\phi = 270°$, the plane containing k_1 and k_2 also contains the [001] axis.

The solid line is a plot of Eq. (4.3) using Waterman's values of A and B. There are no adjustable parameters in this theory. Thus Fig. 8 provides quantitative confirmation of the theory for the [110] direction of cubic materials.

We have also studied the change in amplitude of the hf input wave as a result of the interaction. It was shown in Sec. II that this change should be proportional to the initial amplitude of the hf input wave and to the square of the initial amplitude of the lf input wave. Experimental verification of these dependencies is shown in Figs. 9 and 10. For these data the sample was fused quartz and the input frequencies were 300 and 20 Mc/sec. Note that some saturation is evident in Fig. 9. The highest amplitude point in Fig. 9 corresponds to a change in hf amplitude of about −3 dB. By going to 500 Mc/sec in this sample, a −7 dB change
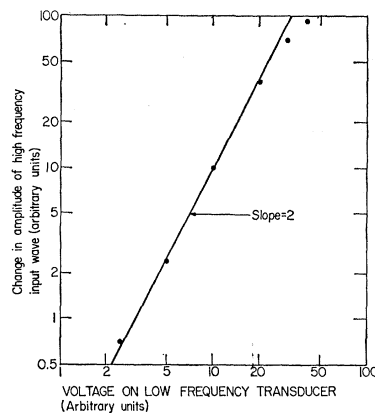

FIG. 9. Change in amplitude of high-frequency input wave as a function of the amplitude of the low-frequency input wave.

was observed. It is not surprising that the perturbation theory treatment breaks down for effects this strong. Data similar to Figs. 9 and 10 have been reported by Shiren.[7] We have also verified that the angular dependence of the change in amplitude of the hf input wave is given by F^2 as predicted by Eq. (2.16). No measurements of the change in amplitude of the lf input wave have been made, since the small transit time across the water gap in our apparatus and the occurrence of multiple reflections in the water prevent gating out a single lf echo.

We have thus experimentally confirmed most of the major features of the theory presented in Sec. II. In particular, the zeros of the interaction which are the most significant experimental points, show the expected dependence on both polar and azimuthal angles.
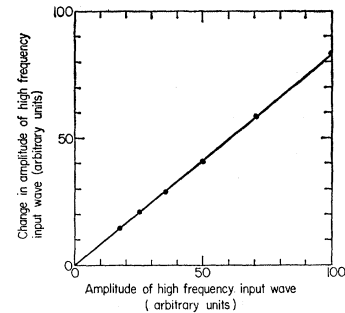

FIG. 10. Change in amplitude of high-frequency input wave as a function of the initial value of this amplitude.

V. SUMMARY AND CONCLUSIONS

In the experiments described in this paper we have simulated the type of three-phonon interaction which is believed to be important in the attenuation of longitudinal ultrasonic waves at low temperatures by replacing the thermal phonons with a coherent ultrasonic wave. In order to ensure the appropriateness of the analogy, the ultrasonic wave which represented the thermal phonons had a much higher frequency than the wave which represented the ultrasonic wave in an attenuation experiment. Also the condition $\omega_1 \tau > 1$ was satisfied in our experiments in analogy to the condition $\omega \tau_{th} > 1$ in an attenuation experiment.

We then inquired what special features might be introduced by replacing an incoherent phonon with a coherent wave. The results of a calculation based on the quantum mechanical coherent state formalism were presented, showing that, neglecting spontaneous emission effects, the square of the amplitude of the sum- or difference-frequency wave in our experiment behaved the same way as the energy in the sum- or difference-frequency mode for incoherent interactions. In particular the angular dependence was found to be the same as that obtained both from the incoherent quantum-mechanical calculation and from the purely classical formulation due to Armstrong *et al.* Other differences between the coherent and incoherent cases

arose in considering the change in amplitude of one of the input waves as a result of the interaction. We next discussed the effect of damping on sum- or difference-frequency generation. We found that the angular dependence could be nearly the same as in the lossless case even when the mean free time of the input wave γ_2^{-1} was less than the transit time across the sample. This result, although intuitively surprising, was borne out by the experimental observations.

We have presented data on the sum- or difference-frequency amplitude as a function of the angle between the input waves, the frequency of the lf input wave and the orientation of the plane of interaction relative to the crystallographic axes. We have also studied the change in amplitude of the hf input waves as a function of the angle between the input waves and of the initial amplitudes of the two input waves. All of these data were in good agreement with the theoretical predictions.

An important result of this investigation is the verification of the theory for interactions in an anisotropic medium. Our technique has provided a successful check of Waterman's theory of elastic anisotropy, a theory which has wide applicability.

ACKNOWLEDGMENTS

APPENDIX: CALCULATION OF $\Delta\omega_\pm$

The calculation presented here closely parallels that of Ciccarello and Dransfeld.[32] However, they considered an isotropic medium and assumed that $\omega_2 \gg \omega_1$. Those restrictions are removed here. The only approximation made in this calculation is that the angles involved are small.

$\Delta\omega_\pm$ is defined by

$$\Delta\omega_\pm = \omega_2 \pm \omega_1 - \omega_\pm, \qquad (A1)$$

where ω_1 is the lower input frequency, ω_2 is the higher input frequency, and $\omega_\pm$ is the generated frequency. The ω's are related to the corresponding wave vectors

[32] I. S. Ciccarello and K. Dransfeld, Phys. Rev. **134**, A1517 (1964).

(see Fig. 3) by

$$\omega_1 = v(\theta)k_1,$$
$$\omega_2 = v_0 k_2, \qquad (A2)$$
$$\omega_\pm = v(\psi)k_\pm,$$

where k_i is the magnitude of the vector $\mathbf{k}_i$, and $v(\theta)$ is the phase velocity of a wave at an angle θ to a particular pure-mode axis. It is assumed that $\mathbf{k}_2$ lies along this pure-mode axis but the same results can be obtained, in the small-angle approximation, if $\mathbf{k}_1$ lies along this axis. v_0 is the phase velocity along the pure-mode axis. Waterman[26] has shown that for many cases $v(\theta)$ may be written, to lowest order in θ, as

$$v(\theta) = v_0(1 - b\theta^2). \qquad (A3)$$

The anisotropy parameter b has been calculated by Waterman from the elastic constants of the material for several crystal symmetries. b may contain a factor depending on the azimuthal angle ϕ but this is unimportant since the three vectors $\mathbf{k}_1$, $\mathbf{k}_2$, and $\mathbf{k}_\pm$ are coplanar. Only the dependence on the polar angle θ interests us here.

We require that wave vector be conserved since otherwise the matrix elements of the interaction Hamiltonian vanish:

$$\mathbf{k}_2 \pm \mathbf{k}_1 = \mathbf{k}_\pm \qquad (A4)$$

or

$$k_\pm^2 = k_2^2 + k_1^2 \pm 2k_1 k_2 \cos\theta$$
$$\approx (k_2 \pm k_1)^2 \mp k_1 k_2 \theta^2, \qquad (A5)$$

where we have assumed that θ is small. Taking the square root of Eq. (A5) and again keeping only lowest order terms in θ, we obtain

$$k_\pm = k_2 \pm k_1 \mp (1/2v_0)\omega_{\mathrm{eff}}^{\pm}\theta^2, \qquad (A6)$$

where

$$\omega_{\mathrm{eff}}^{\pm} \equiv \frac{\omega_1\omega_2}{\omega_2 \pm \omega_1} \approx v_0 \frac{k_1 k_2}{k_2 \pm k_1}. \qquad (A7)$$

Combining Eqs. (A1)–(A3) yields

$$\Delta\omega_\pm = v_0(k_2 \pm k_1 - k_\pm) \mp b\theta^2 v_0 k_1 + b\psi^2 v_0 k_\pm. \qquad (A8)$$

Eliminating ψ by the law of sines (replacing the sine by its argument) and eliminating $k_\pm$ by use of Eq. (A6), we obtain, after a little algebra,

$$\Delta\omega_\pm = (\tfrac{1}{2} - b)\omega_{\mathrm{eff}}^{\pm}\theta^2 + O(\theta^4). \qquad (A9)$$

If $\omega_2 \gg \omega_1$, $\omega_{\mathrm{eff}}^{+} \approx \omega_{\mathrm{eff}}^{-} \approx \omega_1$. Note that $\omega_{\mathrm{eff}}^{-}$ does not actually have a pole if $\omega_2 = \omega_1$, since in that case, ψ would be large and the small-angle approximation would not be valid.